Single-Harmonic Response Open-loop Kelvin-probe Force Microscopy

Thomas Hackl, Mathias Poik, and Georg Schitter

***Abstract*—The measurement of electrical surface charges and their associated potentials at the nanoscale plays a crucial role in understanding important molecular processes, such as corrosion or biological tissue interactions. Measurement of these potential distributions, especially in aqueous environments, is not always possible with standard AFM-based techniques. The herein proposed single-harmonic response open-loop Kelvin-probe Force Microscopy (SH-KPFM) mode circumvents issues of common methods and enables such investigations in water via a suitable choice of the electrical excitation signal. The mode is validated by means of parameter sweeps on calibration samples and compared to conventional KPFM in air. Furthermore, SH-KPFM is applied to investigate the potential distribution and time-dependent depolarization of a charged PMMA surface immersed in deionized water, demonstrating its ability to analyze complex electrostatic interactions on the nanoscale.**

***Index Terms*—Kelvin-probe Force Microscopy, surface charge, solid-liquid interface, PMMA, aqueous solution**

I. Introduction

SURFACE charges and potentials play a key role in various processes ranging from energy conversion/storage [1] to interactions at the biomolecular scale [2]. Gaining further understanding of the underlying mechanisms is of paramount importance and requires knowledge of these electrical sample properties at the nanoscale. The only techniques providing a spatially resolved quantitative measurement thereof are based on Atomic Force Microscopy (AFM), where a cantilever with a sharp tip at its free end is scanned over the sample surface [3]. The electrostatic interaction of this tip with the sample can be measured, leading to various surface properties such as doping concentration [4] or electric potential distribution [5].

The classical mode among the AFM-based electrical characterisation techniques is known as Kelvin-probe Force Microscopy (KPFM) [6]. It enables the simultaneous measurement of sample topography and its surface potential with nanometer resolution. Despite its successful use for the investigation of novel solar-cell technologies [7] or DNA biomolecules [8], its measurement environment is limited to ambient or vacuum conditions due to its use of a dc-bias. However, many scientifically interesting processes, such as corrosion effects or biological tissue interactions, inherently take place at the solid-liquid interface. Unless the measurement solution is not a non-polar solvent [9], the application of KPFM faces limits in these areas. Especially in polar liquids such as water, the used dc-bias between cantilever and sample in KPFM induces electrochemical reactions such as electrolysis [10], [11], inhibiting a controlled measurement environment and can even cause damage to the cantilever and sample.

With the exception of closed-loop AC-KPFM [12], only open-loop methods [13], [14] have been shown to operate in water, since they circumvent the need for this detrimental dc-bias between cantilever and sample during the measurement. These open-loop modes build on the principle of multi-frequency AFM [15], where the surface potential is determined by measuring the cantilever deflection amplitudes at multiple harmonics (usually two) of the excitation signal, and are therefore often referred to as dual-harmonic (DH)-KPFM. In its most basic form the application of the voltage $U_C = a \cdot \sin(\omega t)$ on the cantilever leads to electrostatic forces and therefore deflection amplitudes at ω and 2ω which are measured. With knowledge (i.e. identification/calibration) of the cantilever transfer functions at these frequencies the quantitative surface potential can then be calculated in a post-processing step. However, this necessity for transfer function calibration poses challenges regarding measurement reliability. Possible tip contamination or other changes in the transfer function throughout the measurement due to drift are especially an issue when operating in liquid environments [16], [17], as they can lead to invalid calibrations and therefore erroneous results. In addition, due to the amplitude detection at multiple related frequencies, it is hardly possible to make use of the enhanced Q-factor at cantilever resonances since the detection frequencies (i.e., ω and 2ω) cannot both be placed individually on cantilever resonances. Further developments, which aimed at improving the spatial resolution [18], the drive frequency [19] or the measurement routine [20], [21] have evolved. However, the general principle with the need for knowledge of the cantilever transfer functions and amplitude detection at non-resonances remained.

The contribution of this paper is the development of single-harmonic response open-loop KPFM (SH-KPFM). It enables quantitative surface potential measurements in water via the detection of the cantilever deflection phase at a single frequency. This is achieved by modification of the electrical excitation signal in order to take advantage of frequency mixing. Since the excitation and thus the detection frequency can be freely chosen, the signal-to-noise ratio (SNR) can be maximized by exploiting the Q-factor at the cantilever resonance. The necessity for calibration is reduced down to a single parameter, which minimizes possible influence of drift

This work was financially supported by the Austrian Science Fund FWF (Project Nr. P 31238-N28) and the FFG Production of the Future programme (Project Nr. 883916) of the Austrian BMK. *(Corresponding author: Thomas Hackl.)*
The authors are with the Automation and Control Institute (ACIN), Technische Universität Wien, 1040 Vienna, Austria (e-mail: hackl@acin.tuwien.ac.at).

Pre-Print version of the article: T. Hackl, M. Poik and G. Schitter, "Single-Harmonic Response Open-Loop Kelvin-Probe Force Microscopy,", 2024. DOI: 10.1109/TIM.2024.3366573

during the measurement. After derivation of the theoretical formulations of SH-KPFM in the following section, the mode is experimentally verified by means of parameter sweeps on a calibration sample. The last part deals with the application of SH-KPFM for surface potential measurements on a partially charged poly(methyl methacrylate) PMMA surface in air and water.

II. Single-Harmonic Response Open-loop KPFM

To enable a measurement of the quantitative surface potential distribution $\phi(x,y)$ of a sample via the deflection response of an AFM cantilever at a single frequency, it is necessary to suitably adjust the electrical excitation voltage U_C. The frequency mixing terms of the resulting electrostatic force should coincide with the fundamental harmonics of U_C, which is achieved by the following voltage:

$$U_\mathrm{C} = a \cdot [\sin(\omega t) + \sin(2\omega t)]. \tag{1}$$

The resulting force on the cantilever $F_\mathrm{el} = {}^1\!/_2 \cdot {}^{\partial C}\!/_{\partial z} \cdot (U_\mathrm{C}+\phi)^2$, arising from the electrostatic interaction of U_C and the local surface potential ϕ on the sample is then given by:

$$F_{el} = \frac{1}{2}\frac{\partial C}{\partial z}\begin{Bmatrix} & \phi^2 + a^2 & \\ +2a\phi \cdot \sin(\omega t) & + & a^2 \cdot \cos(\omega t) \\ +2a\phi \cdot \sin(2\omega t) & - & {}^{a^2}\!/_2 \cdot \cos(2\omega t) \\ & - & a^2 \cdot \cos(3\omega t) \\ & - & {}^{a^2}\!/_2 \cdot \cos(4\omega t) \end{Bmatrix}, \tag{2}$$

where ${}^{\partial C}\!/_{\partial z}$ is the capacitance gradient at the tip-sample separation z. The force terms F_ω and $F_{2\omega}$ (second and third row in (2), respectively) are of particular interest as they are composed of an in-phase (sin) and an out-of-phase (cos) component. These excite the following deflections on the cantilever via its transfer functions $G(\omega)$ and $G(2\omega)$:

$$\begin{aligned} A_\omega &= G(\omega)\cdot F_\omega \\ &= X_\omega \cdot \sin(\omega t + \varphi_\omega) + Y_\omega \cdot \cos(\omega t + \varphi_\omega) \\ \hline A_{2\omega} &= G(2\omega)\cdot F_{2\omega} \\ &= X_{2\omega} \cdot \sin(2\omega t + \varphi_{2\omega}) + Y_{2\omega} \cdot \cos(2\omega t + \varphi_{2\omega}), \end{aligned} \tag{3}$$

where $\varphi_\omega = arg[G(\omega)]$ and $\varphi_{2\omega} = arg[G(2\omega)]$ are the cantilever phase responses at the respective frequencies. In order to correctly separate the two components at ω or 2ω as given in (2), φ_ω or $\varphi_{2\omega}$ need to be compensated. This can be done either in a post-processing step or directly by the used amplitude demodulator (i.e. lock-in amplifier) as shown in Fig. 1. To this end, its reference phase $\Theta_\mathrm{Ref.}$ has to be set accordingly (e.g., $\Theta_\mathrm{Ref.} = -\varphi_\omega$) which is achieved by identification of φ_ω prior to the measurement. A direct measurement of the following orthogonal deflection components (X and Y) is therefore enabled:

$$\begin{aligned} X_\omega &= |G(\omega)| \cdot \frac{1}{2}\frac{\partial C}{\partial z}\cdot 2a\phi \\ Y_\omega &= |G(\omega)| \cdot \frac{1}{2}\frac{\partial C}{\partial z}\cdot a^2 \\ \hline X_{2\omega} &= |G(2\omega)| \cdot \frac{1}{2}\frac{\partial C}{\partial z}\cdot 2a\phi \\ Y_{2\omega} &= -|G(2\omega)| \cdot \frac{1}{2}\frac{\partial C}{\partial z}\cdot \frac{a^2}{2} \end{aligned} \tag{4}$$

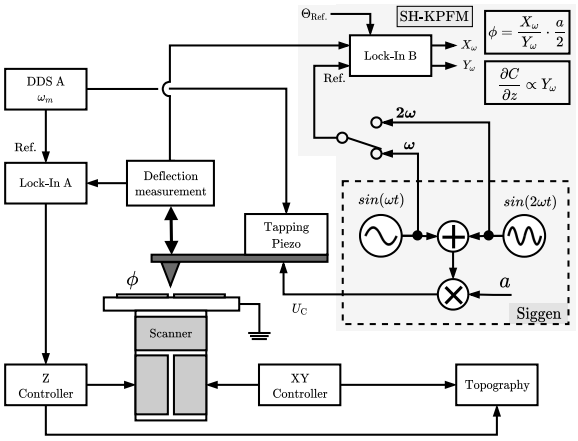

Fig. 1. Setup of SH-KPFM with the added components on the upper right side. A signal generator (dashed box) is used to generate U_C, which is applied to the conducting cantilever. The in-phase and out-of-phase deflection components (i.e., X and Y) are measured by lock-in amplifier B, whose reference frequency is either ω or 2ω. The surface potential ϕ is calculated in a post-processing step as discussed in the text using Equ. (5).

Equ. (4) indicates that the surface potential ϕ can be calculated from the ratio of the in-phase (X) to the out-of-phase (Y) component at either ω or 2ω. The unknown transfer functions $|G(\omega)|$, $|G(2\omega)|$ and the frequency-dependent tip-sample capacitance gradients ${}^{\partial C}\!/_{\partial z}$ at ω and 2ω cancel out:

$$\begin{aligned} \omega: \quad \phi &= \frac{X_\omega}{Y_\omega}\cdot\frac{a}{2} = \cot(\Theta_\omega)\cdot\frac{a}{2} \\ \hline 2\omega: \quad \phi &= -\frac{X_{2\omega}}{Y_{2\omega}}\cdot\frac{a}{4} = -\cot(\Theta_{2\omega})\cdot\frac{a}{4}. \end{aligned} \tag{5}$$

Finally, with the known drive amplitude a and the identity $\cot(\Theta) = {}^X\!/_Y$ follows that the measurement of the demodulated cantilever deflection phase Θ at a single frequency (ω or 2ω) is sufficient for the full quantitative determination of the local surface potential on the sample. However, the measurement of both components is advisable, since Y is directly proportional to the tip-sample capacitance gradient and hence provides additional valuable information on the sample composition [22].

III. Experimental Details

A. Setup

The experimental setup is implemented as illustrated in Fig. 1, where a signal generator (33522B, Keysight Technologies, USA) is used to provide the drive signal U_C to the cantilever and the reference signals (at ω and 2ω) to the external lock-in amplifier (SR844, Stanford Research Systems, USA). The AFM system (Multimode 8, Bruker, USA) consists of a Nanoscope V controller with a signal access module to access various signals, such as the measured cantilever deflection. The inputs of the controller are used to record the demodulated deflection components (X, Y) alongside the topography measurement. With the known drive amplitude

Pre-Print version of the article: T. Hackl, M. Poik and G. Schitter, "Single-Harmonic Response Open-Loop Kelvin-Probe Force Microscopy,", 2024. DOI: 10.1109/TIM.2024.3366573

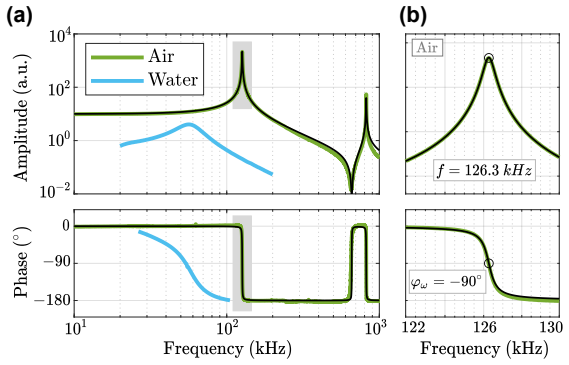

Fig. 2. **(a)** Bode plot of an electrically actuated cantilever in air and water with **(b)** a zoomed-in plot of the first resonance in air as indicated in (a). The working point for SH-KPFM at f_1 for measurements in air is marked with a black circle. Black solid lines represent a model fit considering the first two resonances of the cantilever.

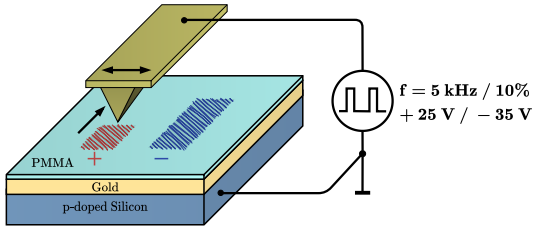

Fig. 3. Charge writing process of the PMMA covered substrate via the application of a pulse-voltage on the AFM cantilever, while scanning in intermittent contact mode over the sample. Two spatially separated regions (10x3.3 µm) are charged with opposing sign as visualized.

a, the surface potential distribution is calculated in a post-processing step using Equ. (5). As conventional KPFM, the instrument is operated in dual-pass mode (i.e. lift-mode) to minimize cross-talk between the topography and surface potential measurements.

For all experiments, the same cantilever (Tap150GB-G, BudgetSensors, Bulgaria) with a nominal stiffness of $k = 5\,\mathrm{N/m}$ and an overall gold coating is used. The noble metal coating ensures good electrical conductivity and prevents any unwanted effects when operating in aqueous solutions (e.g. corrosion of aluminum coated cantilevers). The cantilever is mounted in a liquid-cell holder, that provides a sealed environment to the sample and in-/outlets for liquid exchange. For the experiments in liquid the cell is filled via a connected syringe, containing highly deionized water (milli-Q water, Millipore, USA) [23]. The identified transfer function of the cantilever in air and water is shown in Fig. 2 with a zoomed in view on the first resonance in air together with the marked operation frequency $f = 126.3\,\mathrm{kHz}$. The working point for measurements in water is similarly set on the first resonance at 57 kHz (not highlighted). If not otherwise stated, lift-heights of 50 nm, drive amplitudes of $a = 2\,\mathrm{V}$ and detection at ω is used, which simplifies the calculation of the surface potential down to the relation of the demodulated cantilever deflection amplitudes: $\phi = {}^{X_\omega}/_{Y_\omega}$ (see Equ. (5)).

B. Sample Preparation

For the verification measurements in air in Sec. IV-A a flat n-doped silicon sample is used, whose potential is controlled by a separate signal generator. The applied voltage acts as a ground-truth to which the measured potential is compared.

Measurements on actual spatially distributed surface charges are performed on a flat poly(methyl methacrylate) PMMA covered surface. A gold covered silicon substrate (Micro to Nano, Netherlands) is used as a carrier, onto which a layer of 270 nm PMMA (AR-P 679.04, Allresist, Germany) is spin-coated (checked via ellipsometry). This layer acts as an electret and is subject to charge injection. PMMA is used as it is known for its good charge storage properties, which can even withstand immersion in water [24], [25]. Distributed potential patterns are generated via pulse-voltages between the cantilever tip and the underlying substrate during topography scans as indicated in Fig. 3. To this end a voltage amplifier (WMA-300, Falco Systems, Netherlands), which is controlled by a signal generator is connected to the cantilever. Positive and negative potential areas (10 x 3.3 µm separated by 4 µm) with ~1 V in magnitude are generated via +25 V and -35 V voltage pulses at a repetition rate of 5 kHz and a duty cycle of 10 %, respectively.

C. Measurement Procedure

As already discussed in Sec. II, the phase response of the cantilever at the detection frequency needs to be identified in order to guarantee correct operation. Fig. 2 shows a Bode plot of an electrostatically actuated cantilever, where the first two resonances are clearly visible. Although in general any frequency can be chosen, it is advisable to set the detection frequency (i.e. ω) on a resonance of the cantilever, in order to maximize the sensitivity and the SNR [26]. The step-by-step workflow to perform SH-KPFM measurements is as follows:

1) **Identify** the phase φ_ω by electrostatically actuating the cantilever at the operation frequency → $U_\mathrm{C} = \sin(\omega t)$
   This paper: $\varphi_\omega = -90\,°$
2) **Set the reference phase** of the lock-in amplifier accordingly: $\Theta_\mathrm{Ref.} = -\varphi_\omega = 90\,°$
3) **Operate SH-KPFM** with $U_\mathrm{C} = a \cdot [\sin(\omega t) + \sin(2\omega t)]$ and record the demodulated in-phase and out-of-phase deflection components X_ω and Y_ω, respectively.
4) **Calculate** the surface potential ϕ via Equ. (5).

IV. Results and Discussion

A. Theory verification

The single-harmonic response open-loop KPFM mode as derived in Equ. (4)-(5) is verified by means of parameter sweeps. Fig. 4(a) shows the measured demodulation amplitudes X_ω and Y_ω (i) together with the calculated surface potential ϕ (ii) when sweeping the drive amplitude a for the detection at ω. A model fit using Equ. (4) results in a good overlap of theory and experiment. As for the calculated potential in (ii), it converges to the applied 0.5 V with increasing drive amplitude, demonstrating its quantitative measurement capabilities. Here, the natural contact potential

Pre-Print version of the article: T. Hackl, M. Poik and G. Schitter, "Single-Harmonic Response Open-Loop Kelvin-Probe Force Microscopy,", 2024. DOI: 10.1109/TIM.2024.3366573

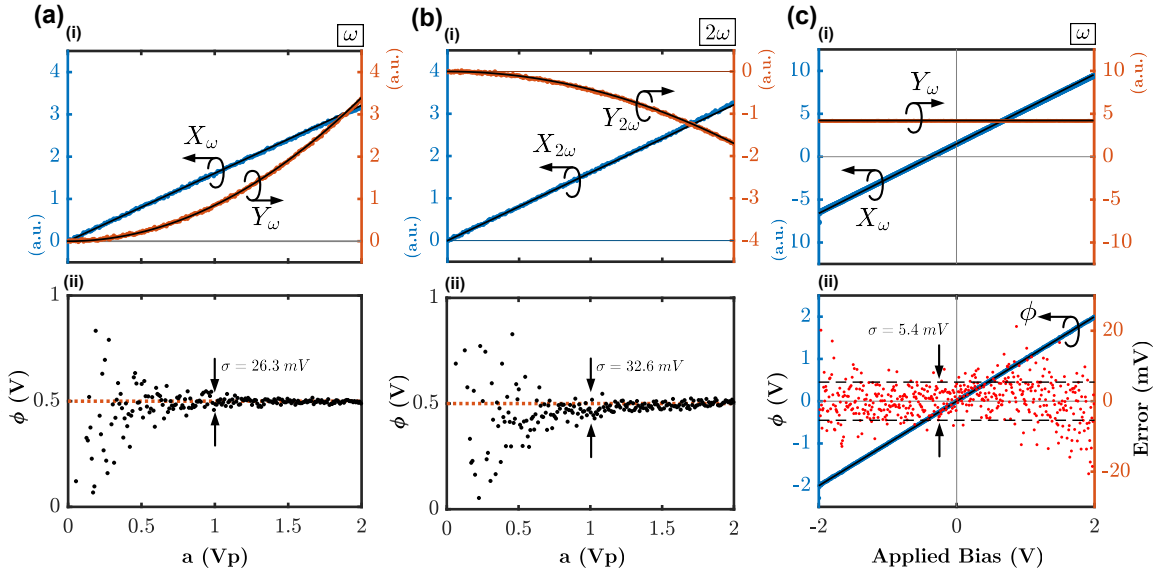

Fig. 4. **(a,b)** Influence of the drive amplitude a on **(i)** the measured in-phase and out-of-phase components (X and Y, respectively) and **(ii)** the calculated surface potential ϕ, when operating with the **(a)** ω and **(b)** 2ω variant of SH-KPFM. Dotted lines in (ii) represent the constant applied sample bias voltage (0.5 V). **(c)** Influence of the applied sample bias on **(i)** the demodulation components and **(ii)** the measured surface potential at a constant drive amplitude a, with the measurement error plotted on the right y axis. Black solid lines represent fitted curves using the model derived in Equ. (4). The calculated surface potential values in (ii) are corrected for the tip-sample CPD to allow a quantitative comparison to the applied sample bias.

difference (CPD) of the tip and sample material (determined in a separate measurement using conventional KPFM) is already taken into account to allow this quantitative comparison. In (b) the same measurement and fit, but with the detection set at 2ω is shown. For this the drive frequency is adjusted to $f = {}^{126.3}/_{2} = 63.15\,\text{kHz}$ to allow a fair comparison (i.e. equal sensitivity via the detection at the same frequency and thus the same cantilever dynamics). Since the Y-component reduces by a factor of 2 when measuring at 2ω as compared to ω (see Equ. (4)) the SNR reduces noticeably. This can can be seen by the increased standard deviation at the same measurement conditions ($a = 1\,\text{V}$). Due to this fact and since there are no differences in instrumentation, the operation of SH-KPFM at ω instead of 2ω is favourable and therefore used in the upcoming experiments. Fig. 4(c)(i) shows the measured demodulation components at ω, when sweeping the applied sample bias voltage at a fixed drive amplitude a. Again, the model fit perfectly overlays with the measured amplitudes. The deviation of the measured surface potential ϕ to the applied potential in (ii) exhibits only a standard deviation of $\sigma = 5.4\,\text{mV}$ over the shown 4 V range, which closely matches the performance of conventional KPFM modes [20].

B. SH-KPFM vs. conventional KPFM

After injecting surface charges in the PMMA covered sample as described in Sec. III-B its topography and surface potential distribution is measured in air and shown in Fig. 5. The surface roughness of the PMMA layer in (a) lies in the single nm range, making it an ideal sample for showcasing SH-KPFM as possible topographical crosstalk is inhibited. The measurement via conventional KPFM in (b) reveals the positively and negatively charged surface areas on the sample. Basically the exact same potential distribution is measured with SH-KPFM via the detection of the amplitudes X_ω and Y_ω (c). Although hardly observable, SH-KPFM features a slightly sharper transition at the edges of the charge rectangles than KPFM. This originates from the fact that, SH-KPFM doesn't incorporate a controller. The response of the cantilever with its predefined Q-factor and resonance frequency [27] is therefore the only limiting factor in terms of scan-speed during SH-KPFM measurements. Furthermore (under the assumption of time-invariant $|G(\omega)|$), the out-of-phase image Y_ω is proportional to the tip-sample capacitance gradient, providing additional information on the sample composition. Since the used PMMA surface is purely homogeneous, the Y_ω image doesn't contain any texture (as expected).

The lift-height dependence of the measured potential at the indicated cross-section is shown in (d). When distancing from the surface the sharp cantilever tip has less proportional influence on the overall electrostatic force, which results in averaging over an increasing sample area [28]. However, even at a tip-sample distance of 1 µm a clear contrast between the individual charge-areas can be seen. This observation changes when immersing the sample in aqueous media, as treated in the following.

C. SH-KPFM operation in water

As discussed in the introduction one major advantage of SH-KPFM is its dc-bias free operation, making it suitable for operation in polar liquids such as water. As shown in Fig. 6,

Pre-Print version of the article: T. Hackl, M. Poik and G. Schitter, "Single-Harmonic Response Open-Loop Kelvin-Probe Force Microscopy,", 2024. DOI: 10.1109/TIM.2024.3366573

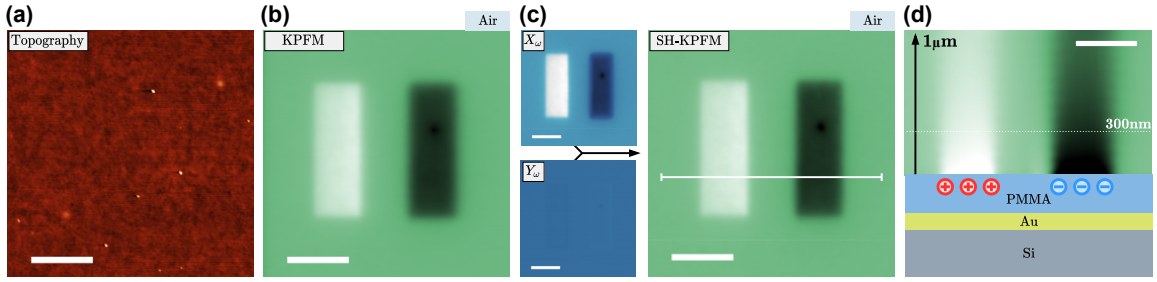

Fig. 5. **(a)** Topography of the partly charged PMMA surface with **(b)** the surface potential distribution measured with conventional KPFM. **(c)** Measured demodulation components (X_ω, Y_ω) with the calculated potential distribution using SH-KPFM on the right. **(d)** Tip-sample distance dependence of the measured surface potential at the scan-line indicated in (c). (measurement environment: air — lift height (b,c): 50 nm — topography color scale: 10 nm — potential color scale: 2 V — scale bar: 5 µm)

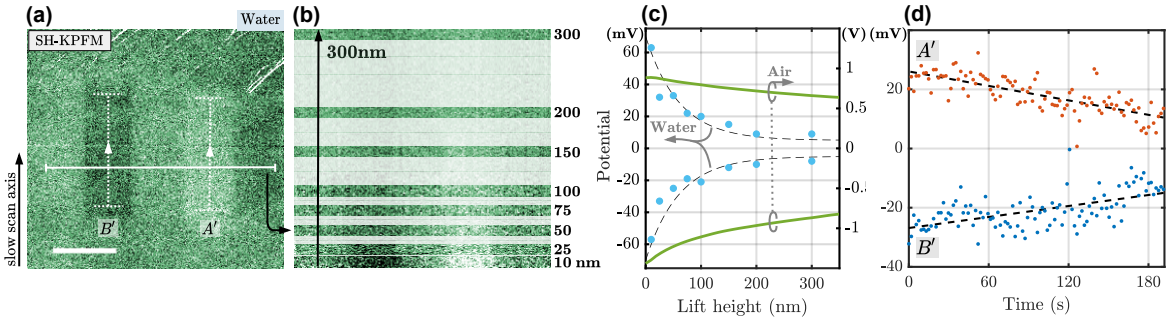

Fig. 6. **(a)** Potential distribution of the charged PMMA surface measured with SH-KPFM in water. **(b)** Lift-height dependence of the measured potential at several specific distances along a single scan-line as indicated in (a). A neutral filler background is added for better visualization. **(c)** Comparison of the measured potentials at the low- and high-side as a function of lift-height in air and water. Dashed lines represent fitted exponential curves with a decay length of 60 nm. **(d)** Dissipation of the surface potential over time due to water-molecule induced depolarization of the PMMA layer. (measurement environment: deionized water — lift height (a): 50 nm — potential color scale: 150 mV — scale bar: 5 µm)

the individual charged areas on the surface can clearly be resolved. One of the notable challenges when operating in water is the highly damped cantilever oscillation (see Fig. 2), resulting in a decreased SNR. The consequences become evident when comparing the measurements in water to those in air (Fig. 6(a) and Fig. 5(c), respectively). Further, upon contact with the water molecules dipole, which feature a random orientation in the bulk solution, the PMMA layer undergoes partial depolarization via the formation of a hydration layer near its surface [16]. This depolarization increases as the water is flushed due to induced turbulent flow inside the liquid cell. Here, the solution is only injected up to the point where the cantilever/sample system is fully immersed, which leads to a roughly tenfold reduction in potential magnitude and further reduces the SNR.

An interesting observation is the inversion of the signs of the charged rectangles. However, this aligns with previous findings of ourselves and others [12], [29], [30]. This phenomenon is mainly attributed to the presence of the electric double layer (EDL), which forms above charged surfaces immersed in ionized liquids. The interplay of water molecules (hydration layers), surface charges and solvated ions cause its formation and influence the electric potential seen by the cantilever. Despite the use of deionized water in the experiment, a finite number of ions may persist due to imperfect filtering, possible contamination (e.g. dissolved CO_2), and self-ionization of water molecules themselves. This has further a substantial impact on the tip-sample distance dependence of the measured potential, as shown in (b). Unlike measurements in air, the surface potential measurement in water exhibits a nearly complete vanishing of potential contrast as the lift-height increases towards 300 nm. While averaging effects play a similar role as in air, this is amplified by the charge-shielding/screening effect generally associated with the EDL [11], [31]. A comparison of the extracted potential values at the center of the charged areas in air and water as a function of the tip-sample distance is shown in (c).

Another interesting aspect is the observed depolarization of the PMMA surface over time. The electric dipoles of the surrounding water molecules, that are moved/rotated by Brownian motion and the scanning cantilever, exhibit a randomly changing orientation that gradually depolarizes the surface. This is manifested by decreasing potential magnitudes over time as shown by the cross-sectional analysis in (d). Similar observations are also made under ambient conditions due to humidity, albeit over significantly longer time-constants, spanning hours to days [32], [33]. To mitigate the effects of this time-dependent charge dissipation on the experiments,

Pre-Print version of the article: T. Hackl, M. Poik and G. Schitter, "Single-Harmonic Response Open-Loop Kelvin-Probe Force Microscopy,", 2024. DOI: 10.1109/TIM.2024.3366573

the measurement time during investigations of lift-height dependence in (b) is minimized. As such, measurements are conducted only at a few specific heights and reduced from high to low (300 nm → 10 nm), resulting in a measurement duration of ~40 s for Fig. 6(b). It is concluded that due to the increase in potential contrast during sample approach, the EDL shielding effect has a much larger impact on the potential distribution than the time-dependent charge dissipation.

In summary, this work demonstrates the development and instrumentation of SH-KPFM for measuring surface charge distributions in air and water, revealing insights into their temporal and spatial variability. Specifically, the charge dissipation of a polarized PMMA surface exposed to deionized water is analyzed. It is found that the electric dipole of surrounding water molecules and residual ions in the solution have a major influence on the measured potential distribution and dissipation. In terms of instrumentation, the calibration process when compared to other open-loop KPFM modes is eased as SH-KPFM merely requires the identification of a single parameter, specifically the cantilever phase response at the operation frequency. This is comparable to the need for feedback-phase calibration within conventional KPFM.

V. Conclusion & Outlook

The proposed single-harmonic response open-loop KPFM technique (SH-KPFM) enables measurements of nanoscale potential distributions in air and water. By suitably adapting the electrical excitation signal, frequency mixing of the electrostatic force terms is achieved. This enables the determination of the sample surface potential via the cantilever deflection measurement at a single frequency. The consequence is that (different from other open-loop KPFM methods) the sensitivity can be maximized by setting the detection frequency on a cantilever resonance. Further, the technique relies merely on the calibration of a single parameter (i.e. the cantilever phase response at the detection frequency), which is comparable to conventional closed-loop KPFM. This results in increased robustness against possible drifts and other parasitic effects. Future work focuses on developing the technique towards fully calibration-free measurements.

Distributed charged areas are injected into a PMMA covered substrate and investigated with SH-KPFM in air and water. The measurements provide quantitative insight into the spatial and temporal variability of the samples surface potential and thus showcase the feasibility of SH-KPFM for analyzing electric charge-driven mechanisms at the nanoscale in aqueous environments.

Acknowledgments

The authors thank Dr. P. Ourednik for spin-coating the provided samples with PMMA.

References

[1] S. V. Kalinin and N. Balke, "Local electrochemical functionality in energy storage materials and devices by scanning probe microscopies: Status and perspectives," *Advanced Materials*, vol. 22, no. 35, pp. E193–E209, 2010.

[2] J. Park, J. Yang, G. Lee, C. Y. Lee, S. Na, S. W. Lee, S. Haam, Y.-M. Huh, D. S. Yoon, K. Eom, and T. Kwon, "Single-molecule recognition of biomolecular interaction via kelvin probe force microscopy," *ACS Nano*, vol. 5, no. 9, pp. 6981–6990, 2011.

[3] G. Binnig, C. F. Quate, and C. Gerber, "Atomic force microscope," *Phys. Rev. Lett.*, vol. 56, pp. 930–933, Mar 1986.

[4] U. Gysin, E. Meyer, T. Glatzel, G. Günzburger, H. Rossmann, T. Jung, S. Reshanov, A. Schöner, and H. Bartolf, "Dopant imaging of power semiconductor device cross sections," *Microelectronic Engineering*, vol. 160, pp. 18–21, 2016.

[5] K. Nakazawa, K. Fukazawa, T. Uruma, G. Hashiguchi, and F. Iwata, "Imaging of an electret film fabricated on a micro-machined energy harvester by a kelvin probe force microscope," *IEEE Transactions on Instrumentation and Measurement*, vol. 71, pp. 1–7, 2022.

[6] M. Nonnenmacher, M. P. O'Boyle, and H. K. Wickramasinghe, "Kelvin probe force microscopy," *Applied Physics Letters*, vol. 58, no. 25, pp. 2921–2923, 1991.

[7] Z. Li, C. Xiao, Y. Yang, S. P. Harvey, D. H. Kim, J. A. Christians, M. Yang, P. Schulz, S. U. Nanayakkara, C.-S. Jiang, J. M. Luther, J. J. Berry, M. C. Beard, M. M. Al-Jassim, and K. Zhu, "Extrinsic ion migration in perovskite solar cells," *Energy Environ. Sci.*, vol. 10, pp. 1234–1242, 2017.

[8] A. K. Sinensky and A. M. Belcher, "Label-free and high-resolution protein/dna nanoarray analysis using kelvin probe force microscopy," *Nature nanotechnology*, vol. 2, no. 10, pp. 653–659, 2007.

[9] A. L. Domanski, E. Sengupta, K. Bley, M. B. Untch, S. A. L. Weber, K. Landfester, C. K. Weiss, H.-J. Butt, and R. Berger, "Kelvin probe force microscopy in nonpolar liquids," *Langmuir*, vol. 28, no. 39, pp. 13 892–13 899, 2012.

[10] L. Collins, S. Jesse, J. I. Kilpatrick, A. Tselev, M. B. Okatan, S. V. Kalinin, and B. J. Rodriguez, "Kelvin probe force microscopy in liquid using electrochemical force microscopy," *Beilstein journal of nanotechnology*, vol. 6, pp. 201–214, 2015.

[11] K.-i. Umeda, K. Kobayashi, N. Oyabu, Y. Hirata, K. Matsushige, and H. Yamada, "Practical aspects of Kelvin-probe force microscopy at solid/liquid interfaces in various liquid media," *Journal of Applied Physics*, vol. 116, no. 13, p. 134307, 10 2014.

[12] T. Hackl, G. Schitter, and P. Mesquida, "Ac kelvin probe force microscopy enables charge mapping in water," *ACS Nano*, vol. 16, no. 11, pp. 17 982–17 990, 2022.

[13] N. Kobayashi, H. Asakawa, and T. Fukuma, "Nanoscale potential measurements in liquid by frequency modulation atomic force microscopy," *Review of Scientific Instruments*, vol. 81, no. 12, p. 123705, 12 2010.

[14] L. Collins, J. I. Kilpatrick, I. V. Vlassiouk, A. Tselev, S. A. L. Weber, S. Jesse, S. V. Kalinin, and B. J. Rodriguez, "Dual harmonic Kelvin probe force microscopy at the graphene–liquid interface," *Applied Physics Letters*, vol. 104, no. 13, p. 133103, 04 2014.

[15] R. Garcia and E. T. Herruzo, "The emergence of multifrequency force microscopy," *Nature Nanotechnology*, vol. 7, no. 4, pp. 217–226, Apr 2012.

[16] T. Fukuma and R. Garcia, "Atomic- and molecular-resolution mapping of solid–liquid interfaces by 3d atomic force microscopy," *ACS Nano*, vol. 12, no. 12, pp. 11 785–11 797, 2018.

[17] G. S. Shekhawat, A. Chand, S. Sharma, Verawati, and V. P. Dravid, "High resolution atomic force microscopy imaging of molecular self assembly in liquids using thermal drift corrected cantilevers," *Applied Physics Letters*, vol. 95, no. 23, p. 233114, 12 2009.

[18] M. Miyazaki, Y. Sugawara, and Y. J. Li, "Dual-bias modulation heterodyne Kelvin probe force microscopy in FM mode," *Applied Physics Letters*, vol. 121, no. 24, p. 241602, 12 2022.

[19] N. Kobayashi, H. Asakawa, and T. Fukuma, "Dual frequency open-loop electric potential microscopy for local potential measurements in electrolyte solution with high ionic strength," *The Review of scientific instruments*, vol. 83, no. 3, p. 033709, 2012.

[20] J. I. Kilpatrick, E. Kargin, and B. J. Rodriguez, "Comparing the performance of single and multifrequency kelvin probe force microscopy techniques in air and water," *Beilstein Journal of Nanotechnology*, vol. 13, pp. 922–943, 2022.

[21] K. Hirata, T. Kitagawa, K. Miyazawa, T. Okamoto, A. Fukunaga, C. Takatoh, and T. Fukuma, "Visualizing charges accumulated in an

Pre-Print version of the article: T. Hackl, M. Poik and G. Schitter, "Single-Harmonic Response Open-Loop Kelvin-Probe Force Microscopy,", 2024. DOI: 10.1109/TIM.2024.3366573

electric double layer by three-dimensional open-loop electric potential microscopy," *Nanoscale*, vol. 10, pp. 14 736–14 746, 2018.
[22] F. C. Salomão, E. M. Lanzoni, C. A. Costa, C. Deneke, and E. B. Barros, "Determination of high-frequency dielectric constant and surface potential of graphene oxide and influence of humidity by kelvin probe force microscopy," *Langmuir*, vol. 31, no. 41, pp. 11 339–11 343, 2015.
[23] T. Hackl, M. Poik, and G. Schitter, "Influence of imaging parameters on afm surface potential measurements in aqueous solutions," in *2022 IEEE 22nd International Conference on Nanotechnology (NANO)*, 2022, pp. 39–42.
[24] P. Mesquida and A. Stemmer, "Attaching silica nanoparticles from suspension onto surface charge patterns generated by a conductive atomic force microscope tip," *Advanced Materials*, vol. 13, no. 18, pp. 1395–1398, 2001.
[25] H. O. Jacobs and G. M. Whitesides, "Submicrometer patterning of charge in thin-film electrets," *Science*, vol. 291, no. 5509, pp. 1763–1766, 2001.
[26] D. Kohl, P. Mesquida, and G. Schitter, "Quantitative ac - kelvin probe force microscopy," *Microelectronic Engineering*, vol. 176, pp. 28–32, 2017.
[27] T. R. Albrecht, P. Grütter, D. Horne, and D. Rugar, "Frequency modulation detection using high-Q cantilevers for enhanced force microscope sensitivity," *Journal of Applied Physics*, vol. 69, no. 2, pp. 668–673, 01 1991.
[28] G. Li, B. Mao, F. Lan, and L. Liu, "Practical aspects of single-pass scan kelvin probe force microscopy," *Review of Scientific Instruments*, vol. 83, no. 11, p. 113701, 2012.
[29] T. Hackl, M. Poik, and G. Schitter, "Heterodyne ac kelvin probe force microscopy for nanoscale surface potential imaging in liquids," *IEEE Transactions on Instrumentation and Measurement*, vol. 72, pp. 1–8, 2023.
[30] S. Lin, M. Zheng, and Z. L. Wang, "Detecting the liquid–solid contact electrification charges in a liquid environment," *The Journal of Physical Chemistry C*, vol. 125, no. 25, pp. 14 098–14 104, 2021.
[31] E. Strelcov, C. Arble, H. Guo, B. D. Hoskins, A. Yulaev, I. V. Vlassiouk, N. B. Zhitenev, A. Tselev, and A. Kolmakov, "Nanoscale mapping of the double layer potential at the graphene–electrolyte interface," *Nano Letters*, vol. 20, no. 2, pp. 1336–1344, 2020.
[32] L. Ressier and V. L. Nader, "Electrostatic nanopatterning of pmma by afm charge writing for directed nano-assembly," *Nanotechnology*, vol. 19, no. 13, p. 135301, feb 2008.
[33] J. Wang, H. Zhang, G.-s. Cao, L.-h. Xie, and W. Huang, "Injection and retention characterization of trapped charges in electret films by electrostatic force microscopy and kelvin probe force microscopy," *physica status solidi (a)*, vol. 217, no. 20, p. 2000190, 2020.

Thomas Hackl received the M.Sc. degree in energy systems and automation technology from TU Wien, Vienna, Austria, in 2020, where he is currently pursuing the Ph.D. degree with the Automation and Control Institute (ACIN).
His primary research interest are on the development of advanced Atomic Force Microscopy measurement modes with the focus on KPFM and mechatronic system design.

Mathias Poik received the M.Sc. degree in energy systems and automation technology from TU Wien, Vienna, Austria, in 2017, where he is currently pursuing the Ph.D. degree with the Automation and Control Institute (ACIN).
His primary research interests are on the development of electrical Atomic Force Microscopy measurement modes, mechatronic system design, and the control of piezoelectric transducers.

Georg Schitter received the M.Sc. degree in electrical engineering from TU Graz, Graz, Austria, in 2000, and the M.Sc. and Ph.D. degrees from ETH Zürich, Zürich, Switzerland, in 2004.
He is currently a Professor for advanced mechatronic systems at the Automation and Control Institute (ACIN), TU Wien, Vienna, Austria. His primary research interests are on high-performance mechatronic systems, particularly for applications in the high-tech industry, scientific instrumentation, and mechatronic imaging systems, such as AFM, scanning laser, and LIDAR systems, telescope systems, adaptive optics, 3-D printing, and lithography systems for semiconductor industry.
Dr. Schitter received the Journal Best Paper Award of the IEEE/ASME TRANSACTIONS ON MECHATRONICS in 2017, the IFAC Mechatronics from 2008 to 2010, and the Asian Journal of Control from 2004 to 2005, and the 2013 IFAC Mechatronics Young Researcher Award. He served as an Associate Editor for IFAC Mechatronics, Control Engineering Practice, and the IEEE TRANSACTIONS ON MECHATRONICS.

Pre-Print version of the article: T. Hackl, M. Poik and G. Schitter, "Single-Harmonic Response Open-Loop Kelvin-Probe Force Microscopy,", 2024. DOI: 10.1109/TIM.2024.3366573